Thermal Bioclimatic Indicators over Southeast Asia: Historical Status and Future Projections using CMIP6

Mohammed Magdy Hamed[1,3] *, Mohamed Salem Nashwan[2], Shamsuddin Shahid[3], Tarmizi bin Ismail[3], Ashraf Dewan[4], Md Asaduzzaman[5]

[1]Construction and Building Engineering Department, College of Engineering and Technology, Arab Academy for Science, Technology and Maritime Transport (AASTMT), B 2401 Smart Village, 12577, Giza, Egypt. E-mail: eng.mohammedhamed@aast.edu

[2]Construction and Building Engineering Department, College of Engineering and Technology, Arab Academy for Science, Technology and Maritime Transport (AASTMT), 2033 Elhorria, Cairo, Egypt. E-mail: m.salem@aast.edu

[3]Department of Water and Environmental Engineering, School of Civil Engineering, Faculty of Engineering, Universiti Teknologi Malaysia (UTM), 81310 Skudia, Johor, Malaysia. E-mail: sshahid@utm.my (S.S.), tarmiziismail@utm.my (T. I.)

[4]Spatial Sciences Discipline, School of Earth and Planetary Sciences, Curtin University, Kent Street, Bentley, Perth 6102, Australia, E-mail: A.Dewan@curtin.edu.au

[5]Department of Engineering, School of Digital, Technologies and Arts, Staffordshire University, Stoke-on-Trent ST4 2DE, UK, E-mail: Md.Asaduzzaman@staffs.ac.uk

*Corresponding Author E-mail: eng.mohammedhamed@aast.edu

Thermal Bioclimatic Indicators over Southeast Asia: Historical Status and Future Projection CMIP6

Abstract

Mapping potential changes in bioclimatic characteristics are critical for planning climate change adaptation and mitigation goals. Assessment of such changes is particularly important for Southeast Asia, which has one of the world's highest ecological diversity. Twenty-three CMIP6 GCMs are used in this study to evaluate the change in 11 thermal bioclimatic indicators of Southeast Asia for two shared socioeconomic pathways (SSPs), 2-4.5 and 5-8.5. The spatial changes in the ensemble mean, 5th, and 95th percentile of each indicator for the near (2020-2059) and far (2060-2099) futures for the two SSPs to understand the changes with time and associated uncertainty. The results indicate large spatial heterogeneity and temporal variability in projected changes in bioclimatic indicators. A higher change was projected in the mainland SEA for the far future and less in maritime SEA for the near future. At the same time, uncertainty in the projected bioclimatic indices was higher for mainland SEA than maritime SEA. The multimodel ensemble mean (MME) revealed a change in mean temperature in the range of -0.71 to 3.23 °C for the near and 0.00 to 4.07 °C for the far future. The diurnal temperature range was projected to reduce over most of SEA in the range of -1.1 to -2.0 °C, while isothermality to decrease by -1.1 to -4.6%. The decrease in isothermality along with a decrease in seasonality indicates a possible shift in climate, particularly in the north of mainland-SEA in the future. Maximum temperature in the warmest month/quarter was projected to increase a little more than the coldest month/quarter and the mean temperature in the driest month to increase more than the wettest month. This would cause an increase in the annual temperature range in the future.

Keywords: CMIP6, GCM, SEA, Bioclimatic indicators, climate change,

1. Introduction

Annual and seasonal bioclimate information is essential to understand climate influences on different species (O'Donnell and Ignizio, 2012). It is also required to estimate wildlife distribution (Molloy et al., 2014; Yoon and Lee, 2021), farming potential (Kriticos et al., 2012), human comfort (Çaliskan et al., 2013) and climate change vulnerability (Theusme et al., 2021). Global warming has altered climate in different ways in different regions of the globe. Climate change has changed several climatic characteristics intricately connected to the biosphere (Pour et al., 2019). Minor climate changes may significantly affect biological distribution (Hu et al., 2015; Sintayehu, 2018), such as a shift in species distribution and ecology as the plants and animals would change their locations with the climate for survival (Bellard et al., 2012; Molloy et al., 2014; Waltari et al., 2014). The phenology and physiology of many plants may also change in response to climate variability (Bellard et al., 2012). It would also alter people's comfort and public health risk in different regions (Duanmu et al., 2017; Ragheb et al., 2016).

Bioclimatic indicators are increasingly being used to analyze the effects of climate change on bio-environments (Daham et al., 2018; Rehfeldt et al., 2015; Ribeiro et al., 2019). Mapping potential changes in bioclimatic characteristics are critical for achieving climate change adaptation and mitigation goals. Bioclimatic indicators' historical and future projection is particularly important for the Southeast Asia (SEA) region. SEA is the world's most climate-vulnerable area due to significant ocean-land-atmosphere interactions (Raitzer et al., 2015; Vinke et al., 2017). It is in the center of the Asian monsoon system and at the crossroads of the Asian monsoon's interactions with the El Niño–Southern Oscillation (ENSO), the Pacific and Indian Oceans and the Northern and Southern Hemispheres. Four SEA nations are rated among the world's ten most susceptible countries to climate change (Eckstein et al., 2017). According to a recent study (Raitzer et al., 2015), the SEA region's gross domestic product will decline by 11% by the end of the current century as a result of the negative effects of climate change, the highest rate on the planet. Agriculture and ecological industries would be the two most affected. Crop yields will drop significantly as a result of the changing climate on the land surface. Significant biome shifts might have a detrimental effect on ecosystems and the livelihoods of millions (Woetzel et al., 2020).

Several studies assess the distribution of plants (Banerjee et al., 2019; van Zonneveld et al., 2009) in SEA and others assess the distribution of animals due to climate change (Abdullah, 2003; Rauff-Adedotun et al., 2020). Asif (2019) studied the environmental impact on marine resources, especially the fishing industry on Cambodia's coast, and its impact on the migration of citizens. Yoon and Lee, (2021) used the bioclimatic indicators to study the distribution of two different pests using MaxEnt modeling. Besides, scientists used Global Climate Models (GCMs) to assess climate change impacts on biodiversity (Flato et al., 2013; Hartmann, 2016). Dai et al., (2021) studied the impact of climate change on the distribution of two different bears using CMIP5 at current and far future (2070) in China. Wang et al., (2021) studied the projected future distribution of six species of flowering plants using Species Distribution Models (SDMs) in current, 2050, and 2070 using CMIP5 medium (RCP4.5) and high (RCP8.5) scenarios. Thus, assessing the bioclimatic indicators in historical and future scenarios across SEA is critical for the region's sustainable development.

A more realistic representation of Earth's physical processes is included in the most recent CMIP6 than prior CMIPs (Eyring et al., 2016) using more robust future scenarios known as Shared Socioeconomic Pathways (SSPs) (Moss et al., 2010; Taylor et al., 2012). These SSPs examine future climate change and global economic and demographic shifts, at eight different degrees, namely SSP1-1.9, SSP1-2.6, SSP2-4.5, SSP3-7.0, SSP4-3.4, SSP4-6.0, SSP5-3.4 and SSP5-8.5. Historical and future projections of CMIP6 GCMs were found to have less uncertainty than previous versions (Almazroui et al., 2020; Deng et al., 2021; Ombadi et al., 2020).

The purpose of this work is to quantify historical bioclimatic indicators and their future change in SEA under medium and high climate change scenarios. Thus, eleven thermal bioclimatic indicators were estimated for the historical period and the future until the end of the century using the SSP2-4.5 and SSP5-8.5 scenarios derived from a multi model ensemble mean of 23 CMIP6 GCMs. The study's novel is the use of readily available climate projection data to assess possible changes in bio environment in two future periods and two climate change scenarios. Additionally, it may be used to assist decision-makers and policymakers in developing future climate change mitigation and adaptation strategies in the SEA.

2. Study Area and Data

2.1. Study Area

SEA consists of 11 countries having a 563 million population and a land area of 4.3 million km^2 (Fig. 1). With 173,251 kilometers of coastline, it ranks third worldwide, after North

America and Western Europe. There are seas, land, and many islands in SEA, consisting of two primary regions (i.e., Mainland and Maritime SEA). Most of SEA's topography is flat, except for Myanmar and Indonesia, where altitudes surpass 4000 meters. SEA is one of the world's most vulnerable regions to climate change because of its unique geographic and meteorological conditions and economic, demographic, and social features (Raitzer et al., 2015; Vinke et al., 2017). It has a mean annual temperature of 25.0 °C and a mean annual rainfall between 700 and 5000 mm (Peel et al., 2007; Yang et al., 2021). The natural atmospheric processes that cause climate-related catastrophes, such as droughts, floods, and other weather events, operate on a spectrum of spatial and temporal variability (Kuo et al., 2020; Nashwan et al., 2018).

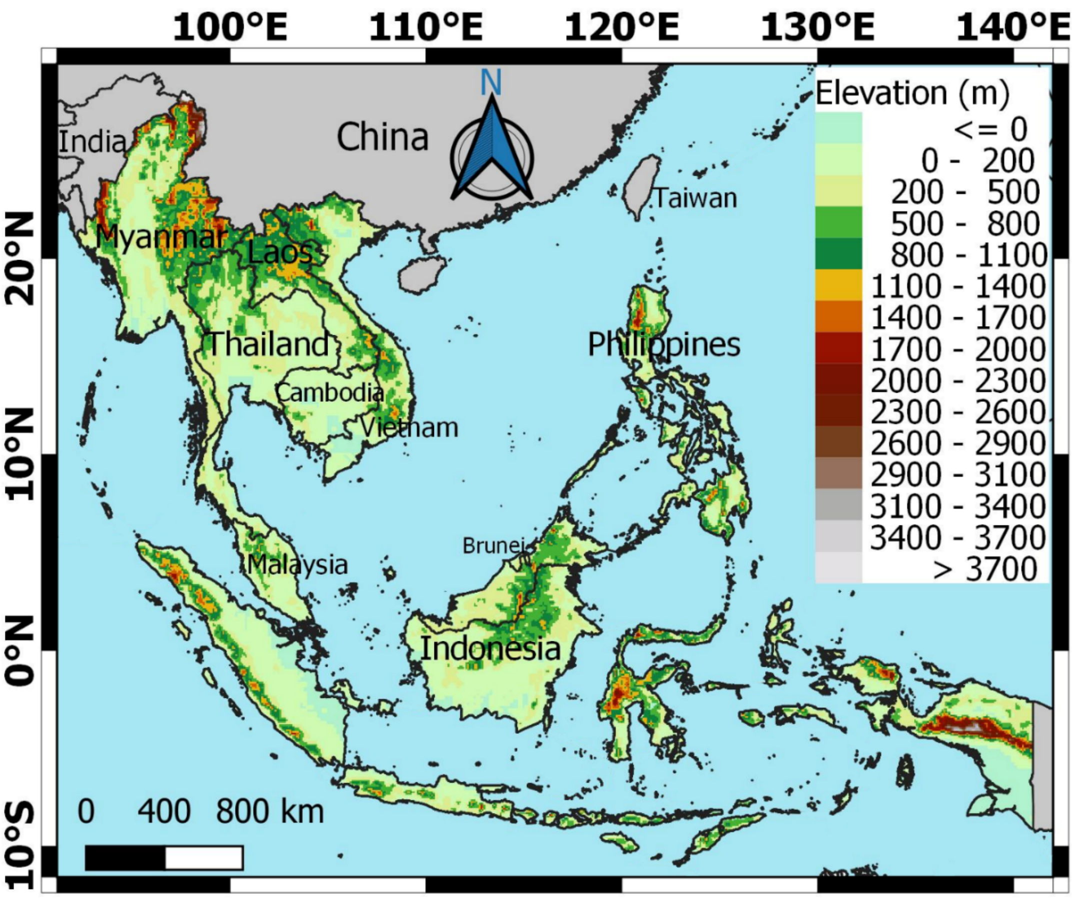

Fig. 1 The location and topography of Southeast Asia

2.2. Global Climate Models

Twenty-three CMIP6 models' monthly rainfall, T_{max} and T_{min} simulations for the historical and future periods were used. The GCMs (Table 1) were chosen based on the availability of projections for rainfall, T_{max} and T_{min} for the historical, and two SSPs, 2-4.5 and 5-8.5. The models' outputs were acquired via https://esgf-node.llnl.gov/search/cmip6/. Only the outputs of the initial variation label r1i1f1p1 were considered out of different initializations of each GCM. The historical experiment covers the period 1975 – 2014, while the future experiments (i.e., SSP2-4.5 and SSP5-8.5) cover 2020 - 2099. The SSP2-4.5 scenario implies the middle of the road scenario, which mean global temperature will reach 2.7°C by 2100. Contrarily, SSP5-8.5 represents the worst-case future scenario with double CO_2 emissions levels by 2050 compared to the current level and a global temperature warming of 4.4°C by the end of the century. Thus, employing these two future scenarios can reflect the variability in possible pathways of climate warming.

Table 1 CMIP6 GCMs used in the study

No	Model	Institution	Country	Raw Nominal Resolution (km)	Reference
1	ACCESS-CM2	CSIRO-ARCCSS	Australia	250	(Dix et al., 2019)
2	ACCESS-ESM1-5			250	(Ziehn et al., 2019)
3	AWI-CM-1-1-MR	AWI	Germany	100	(Semmler et al., 2018)
4	BCC-CSM2-MR	BCC	China	100	(Wu et al., 2018)
5	CanESM5	CCCMA	Canada	500	(Swart et al., 2019)
6	CAS-ESM2-0	CAS-ESM	China	100	(Chai, 2020)
7	CIESM	CIESM	China	100	(Huang, 2019)
8	CMCC-ESM2	CMCC	Italy	100	(Peano et al., 2020)
9	EC-Earth3	EC-Earth	Europe	100	(Döscher et al., 2021)
10	EC-Earth3-CC			100	
11	EC-Earth3-Veg			100	
12	EC-Earth3-Veg-LR			100	
13	FGOALS-g3	FGOALS	China	250	(Pu et al., 2020)
14	FIO-ESM-2-0	FIO	China	100	(Song et al., 2019)
15	GFDL-ESM4	NOAA-GFDL	USA	100	(Krasting et al., 2018)
16	INM-CM4-8	INM	Russia	100	(Volodin et al., 2019a)
17	INM-CM5-0			100	(Volodin et al., 2019b)
18	IPSL-CM6A-LR	IPSL	France	250	(Boucher et al., 2018)
19	MIROC6	MIROC	Japan	250	(Tatebe et al., 2019)
20	MPI-ESM1-2-HR	MPI-M	Germany	100	(von Storch et al., 2017)
21	MPI-ESM1-2-LR			250	(Wieners et al., 2019)
22	MRI-ESM2-0	MRI	Japan	100	(Yukimoto et al., 2019)
23	NESM3	Nanjing University	China	250	(Cao and Wang, 2019)

3. Methodology

This study explores the change of biothermal indicators in SEA for different future scenarios. Table 2 provides comprehensive explanations of the eleven indicators used. Except for Bio-3 and Bio-4, all indications are in °C. Bioclimatic indicators collect data on annual circumstances (annual mean temperature, annual temperature range), along with seasonal average climate conditions (temperature of the coldest and warmest months). Thus, these indicators with biological significance could help researchers better understand species reactions to climate change (Pour et al., 2019). The methodology flow of work starts with the interpolation of models' outputs into a common 1.0° spatial grid using bilinear interpolation to guarantee that the study results are not biased due to different spatial representations of raw GCMs (refer to Table 1). Then, different indicators were computed for each model output for the historical period and two future scenarios. A multimodel ensemble (MME) was created using the available 23 GCMs' outputs to decrease the uncertainty in projections. The MME mean was then computed as well as the projected change in futures. The future period was divided into two (e.g., near 2020-2059 and far 2060-2100) to address the transition in future estimates.

Table 2 Definitions of the thermal bioclimatic indicators where T_{avg} is the mean temperature $((T_{max}+T_{min})/2)$, and i is the month of the year.

Indicator	Equation	Unit
Bio-1 Annual mean temperature	$Bio1 = \frac{\sum_{i=1}^{i=12} Tavg_i}{12}$	°C
Bio-2 Diurnal temperature range	$Bio2 = \frac{\sum_{i=1}^{i=12}(Tmax_i - Tmin_i)}{12}$	°C
Bio-3 Isothermality	$Bio3 = \frac{Bio2}{Bio7} \times 100$	%
Bio-4 Temperature variation within a year	$Bio4 = SD\{Tavg_1, \dots, Tavg_{12}\} \times 100$	%
Bio-5 Maximum monthly temperature	$Bio5 = \max(\{Tmax_1, \dots, Tmax_{12}\})$	°C
Bio-6 Minimum monthly temperature	$Bio6 = \min(\{Tmin_1, \dots, Tmin_{12}\})$	°C
Bio-7 Annual temperature range	$Bio7 = Bio5 - Bio6$	°C
Bio-8 Mean temperature of wettest quarter	$Bio8 = \frac{\sum_{i=1}^{i=3} Tavg_i}{3}$	°C
Bio-9 Mean temperature of driest quarter	$Bio9 = \frac{\sum_{i=1}^{i=3} Tavg_i}{3}$	°C
Bio-10 Mean temperature of warmest quarter	$Bio10 = \frac{\sum_{i=1}^{i=3} Tavg_i}{3}$	°C

Bio-11 Mean temperature of coldest quarter	$Bio11 = \frac{\sum_{i=1}^{i=3} Tavg_i}{3}$	°C

4. Results

Thermal bioclimatic indicators estimated using different GCMs were used to form an MME. The following sections present the historical MME mean of each indicator. Besides, the projected changes in the mean, 5th, and 95th percentile for each indicator for the near and far futures for SSP2-4.5 and SSP5-8. 5 are presented.

4.1. Annual mean temperature (Bio-1)

The spatial distribution of Bio-1 at different grids over SEA is presented in Fig. 2. The Bio-1 in SEA ranges between 20.0 and 28.0 °C, except for the far north, where it is as low as 2.0°C. Topography had a significant impact on the spatial distribution of Bio-1 over SEA. It is low in the northern and southern mountains and high in the plains. The MME mean of projected Bio-1 revealed an increase of 1.08 and 1.86 °C for the near and far futures for SSP2-4.5. There was almost no difference in the projected changes between the near and far futures (SSP2-4.5) for most Maritime SEA, except for Sarawak, Malaysia. It was projected to increase by 4.0°C above the historical levels for SSP2-4.5 in Mainland SEAs. The areal means of the 5th and 95th percentiles of the projected changes were -0.71 and 3.23 °C for the near future and 0.00 and 4.07 °C for the far future. In the case of SSP5-8.5, the projected MME mean changes in Bio-1 were almost the same as SSP2-4.5 during the near future. However, the changes were expected to increase during the far future by 2.53–4.87 °C. The areal means of 5th and 95th percentiles of the projected changes for SSP5-8.5 were -0.49 and 3.46°C for the near future and 1.17 and 5.50°C for the far future. It indicates more uncertainty in projection for the far future and SSP5-8.5 than the near future and SSP2-4.5

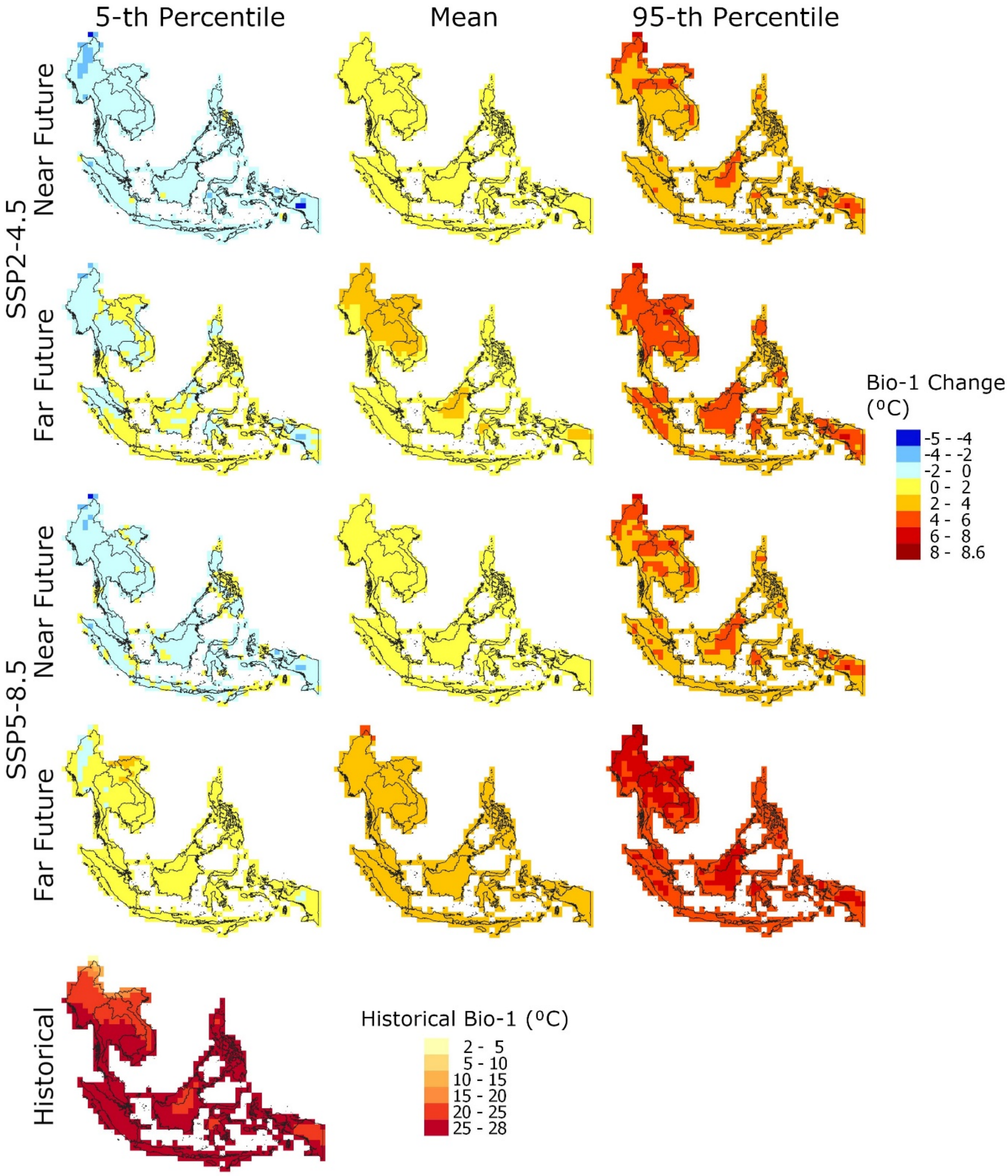

Fig. 2 Spatial distribution of the changes in annual mean temperature (Bio-1) for SSP2-4.5 and SSP5-8.5 in the near and far future: 5th percentile (left), mean (middle) and 95th percentile (right) of 23 GCM projections.

4.2. Diurnal temperature range (Bio-2)

Bio-2 is defined as the difference between daily T_{max} and T_{min}, which significantly impact the ecosystem and public health (Ehbrecht et al., 2019). Due to its position near the equator, the diurnal temperature range (Bio-2) in SEA is low, as seen in Fig. 3. Bio-2 ranged between 1.0

and 11.0°C, with the lowest in the coastal regions of the Maritime SEA and the highest in the far north of Mainland SEA. A higher increase in T_{min} than T_{max}, implying a drop in Bio2 in many locations of the world due to global warming (Karoly et al., 2003; Shahid et al., 2012). The MME projected a mean change in Bio-2 ranging between -0.42 and 0.41 °C for SSP2-4.5, and -0.79 and 0.40 °C for SSP5-8.5, for the near and far futures. There were no significant changes in spatial distribution in mean Bio-2 for future periods. The areal means of the 5th and 95th percentiles of the projected changes for SSP2-4.5 were -2.5 and 3.15 °C for the near future and -2.50 and 3.00 °C for the far future. Besides, they were projected to increase by -2.48 and 3.10 °C for the near future and -2.5 and 2.94 °C for the far future for SSP5-8.5. In addition, there were no major variations in the areal means of 5th and 95th percentiles for different futures.

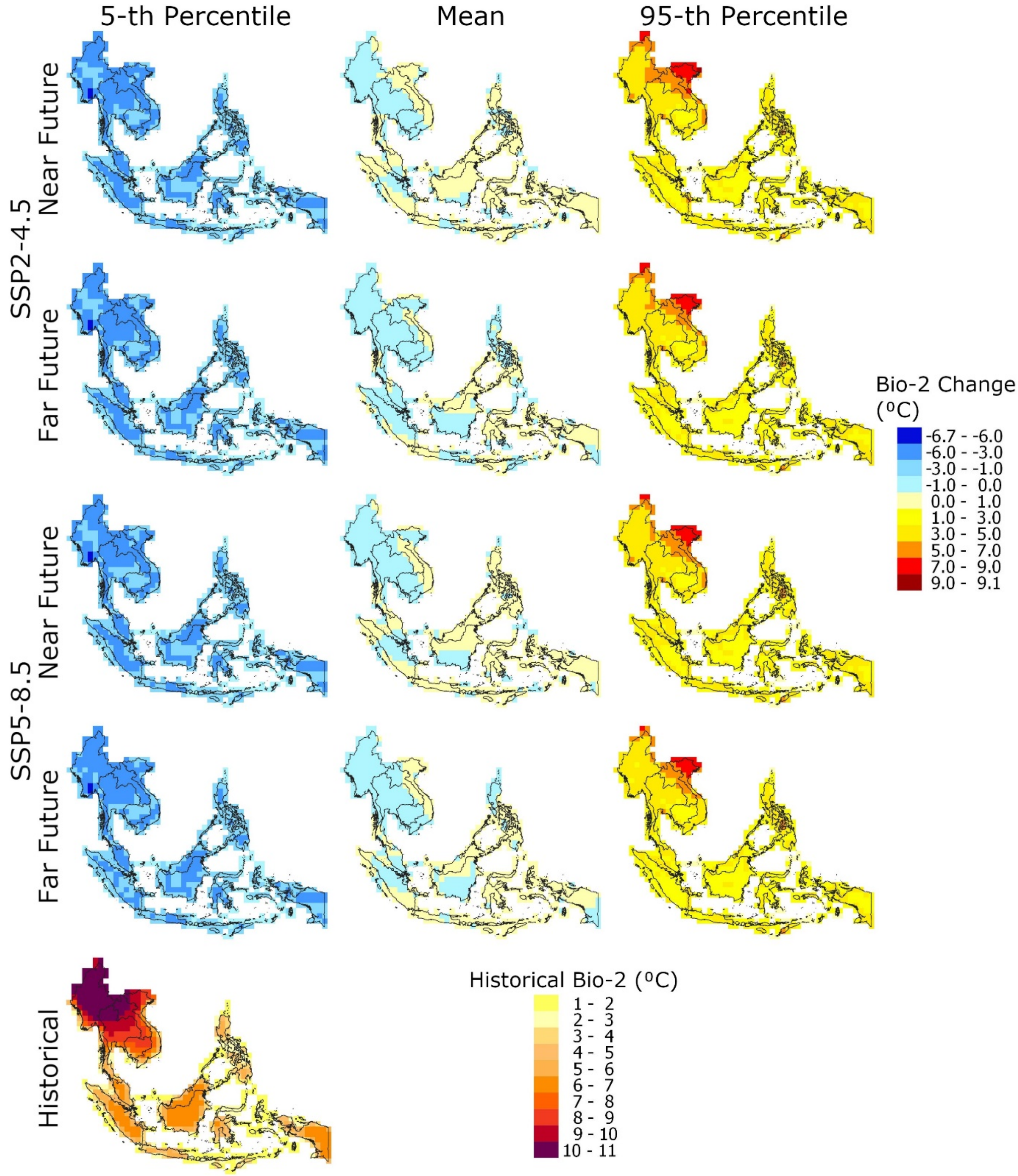

Fig. 3 Spatial distribution of the changes in the diurnal temperature range (Bio-2) for SSP2-4.5 and SSP5-8.5 in the near and far future: 5th percentile (left), mean (middle) and 95th percentile (right) of 23 GCM projections.

4.3. Isothermally (Bio-3)

The spatial distributions of historical Bio-3 and its future projections over SEA are shown in Fig. 4. Bio-3 is the ratio of the annual mean diurnal temperature range (Bio-2) to the annual temperature range (Bio-7). A Bio-3 > 100% indicates smaller diurnal temperature variability as compared to annual temperature variability. It is an essential bioclimatic indicator for SEA because of its tropical topography and maritime environment (Nix, 1986; O'Donnell and Ignizio, 2012). During 1975 – 2014, the mean Bio-3 ranged between 13.0 and 79.0%, as shown in Fig. 4. For SSP2-4.5, the MME mean change ranged between -3.4 and 0.7% during the near future and -4.6 and 1.4% during the far future. Bio-3 mean changes (5th percentile) were estimated to be -14.9 and -15.3% for the near and far future, with the lowest values in the coastal region in the south and central of SEA (i.e., the Philippines). The same regions may also experience a large change in Bio-3 (95th percentile). However, the overall changes would be between 4.47 and 32.82% for the near future and 3.83 and 31.08% for the far future. For SSP5-8.5, the MME mean changes were expected to vary between -3.83 and 0.85% during the near future and -6.91 and 2.10% during the far future. The areal means of 5th and 95th percentiles of projected changes were -15.0 and 13.04% for the near future and -16.03 and 12.20% for the far future. The locations with high Bio-3 in the historical period, like Indonesia and Sarawak in Malaysia, showed the lowest changes for different future scenarios.

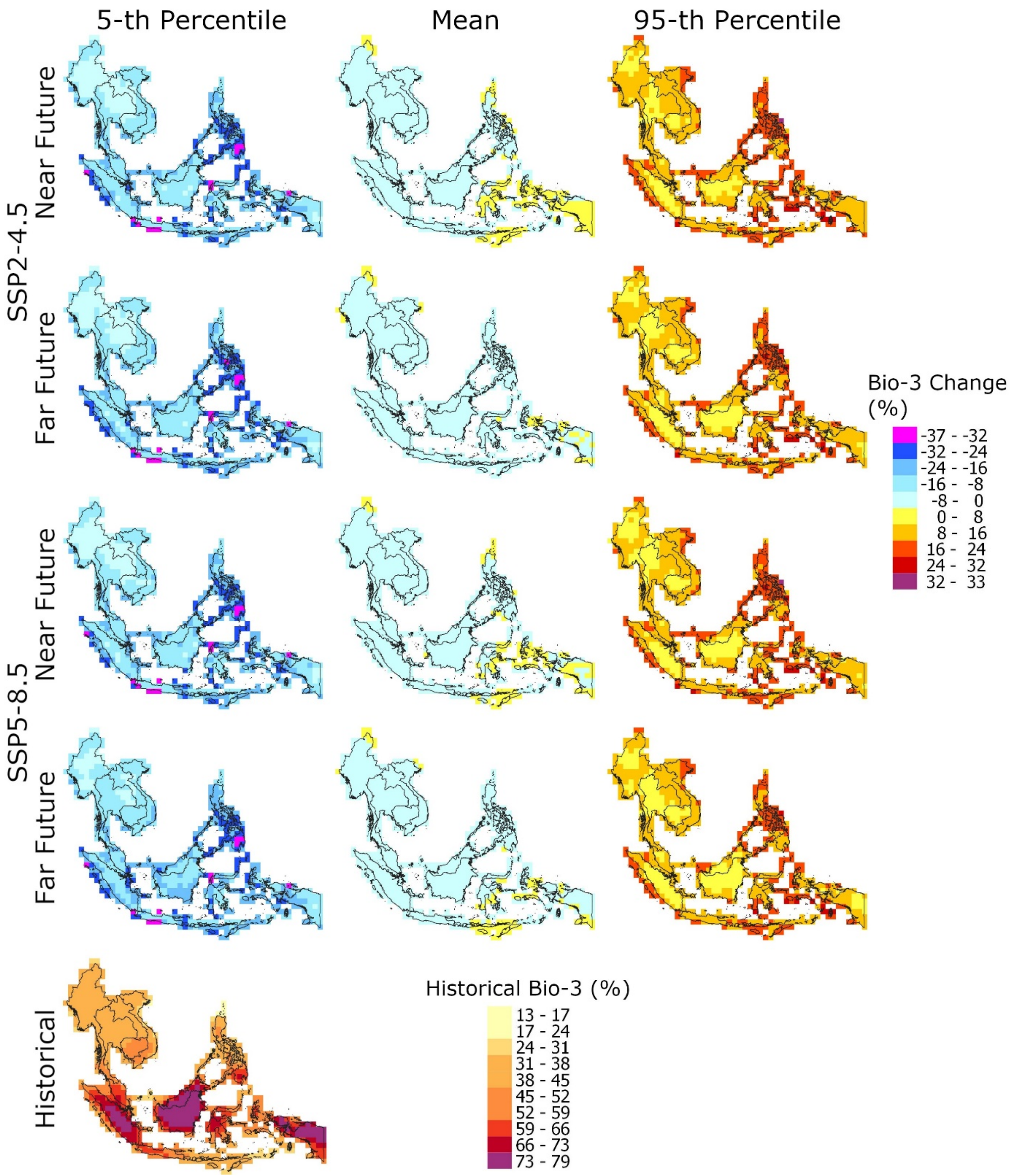

Fig. 4 Same as Figure 3 for isothermally (Bio-3)

4.4. Temperature seasonality (Bio-4)

The seasonality of temperature (Bio-4) is the amount of temperature fluctuation averaged over the years, estimated based on the standard deviation in percentage (O'Donnell and Ignizio, 2012). The historical changes in two future climate projections (SSP2-4.5 and 5-8.5) of Bio-4 are presented in Fig. 5. An increase in Bio-4 indicates a greater variability of temperature fluctuation. The spatial distribution of Bio-4 indicates a non-homogeneous pattern over the SEA. The south of SEA (Indonesia, Malaysia, Brunei, and Singapore) showed the mean Bio-4 of 4.0%, while the north showed nearly 36.0%. Overall, the spatial distribution of projected changes was found the same for different scenarios for the mean, 5^{th,} and 95th percentiles. The MME mean change in Bio-4 was estimated as 1.36% for SSP2-4.5, and 0.70% for SSP5-8.5, for the near future, while 0.40% for SSP2-4.5 and -0.51% for SSP5-8.5 for the far future. The spatial means of the 5th percentile of the projected changes for SSP2-4.5 were estimated as -4.10% for the near future and -4.21% for the far future. Besides, they were projected to change by -4.06% for the near future and -2.52% for the far future for SSP5-8.5. On the other hand, the areal means of 95th percentile was projected to change 2.90% for the near future and 6.31% for the far future for SSP2-4.5, while it was 5.03% for the near future and 2.63% for the far future for SSP5-8.5.

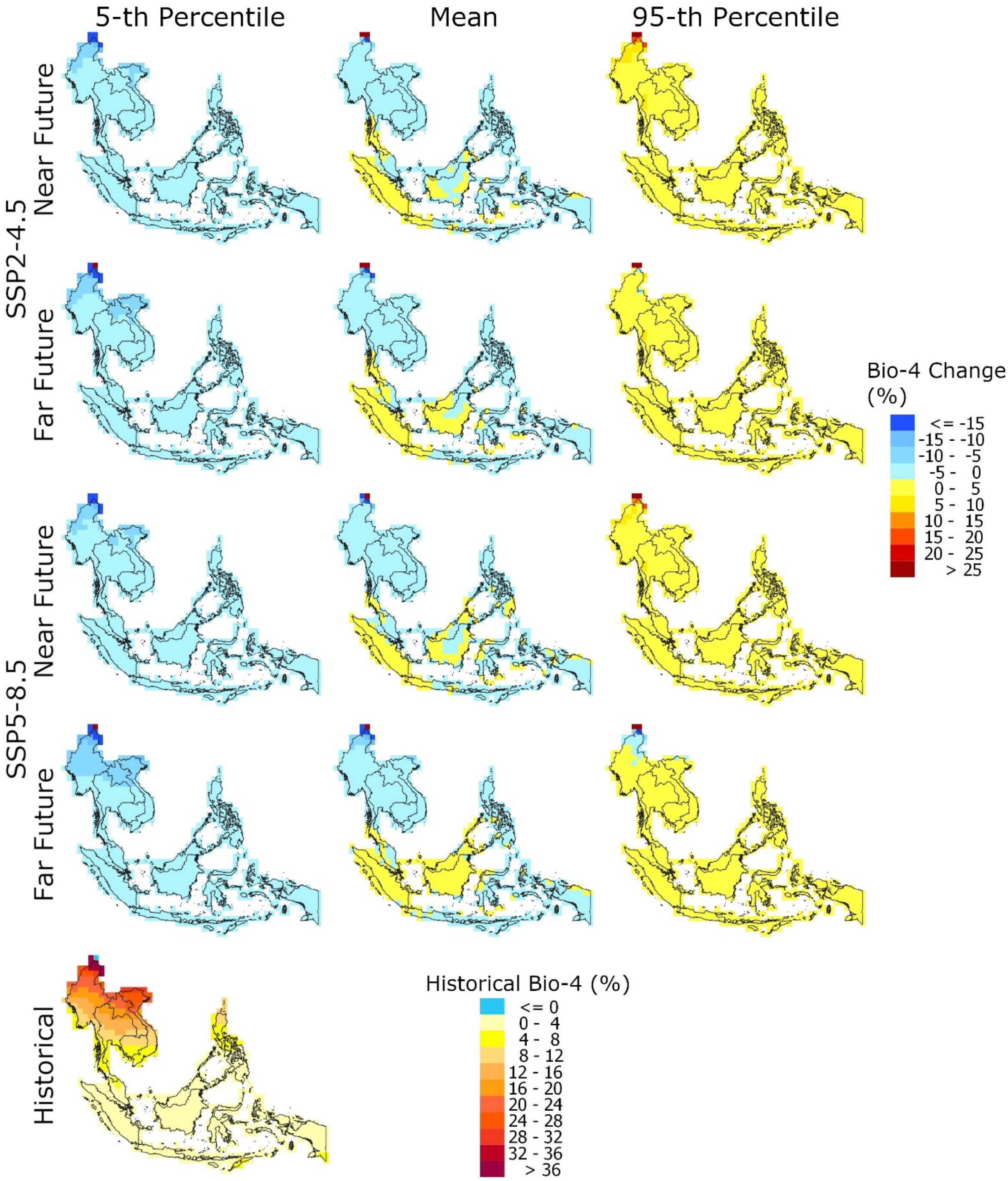

Fig. 5 Same as Figure 3 for seasonality (Bio-4)

4.5. Maximum temperature in the warmest month (Bio-5)

Fig. 6 presents the spatial distribution of maximum monthly temperature (Bio-5) during the historical period over SEA along with two future scenarios (SSP2-4.5 and 5-8.5). The Bio-5 in SEA was ranged between 16.0 and 38.0°C. The highest value was observed in Myanmar and Thailand, while the lowest was in the north of Myanmar. The projected change in mean Bio-5 showed an increase of 1.17 and 1.98 °C for the near and far futures for SSP2-4.5, while 1.35 and 3.27 °C for the near and far futures for SSP5-8.5. The means of 5th and 95th percentiles of the projected changes for SSP2-4.5 were -2.03 and 4.63 °C for the near future and -1.40 and 5.48 °C for the far future. For SSP5-8.5, the means of 5th and 95th percentiles of the projected changes were almost the same as SSP2-4.5 during the near future. However, in the far future, the areal means of 5th and 95th percentiles of the projected changes were -0.29 and 7.07 °C.

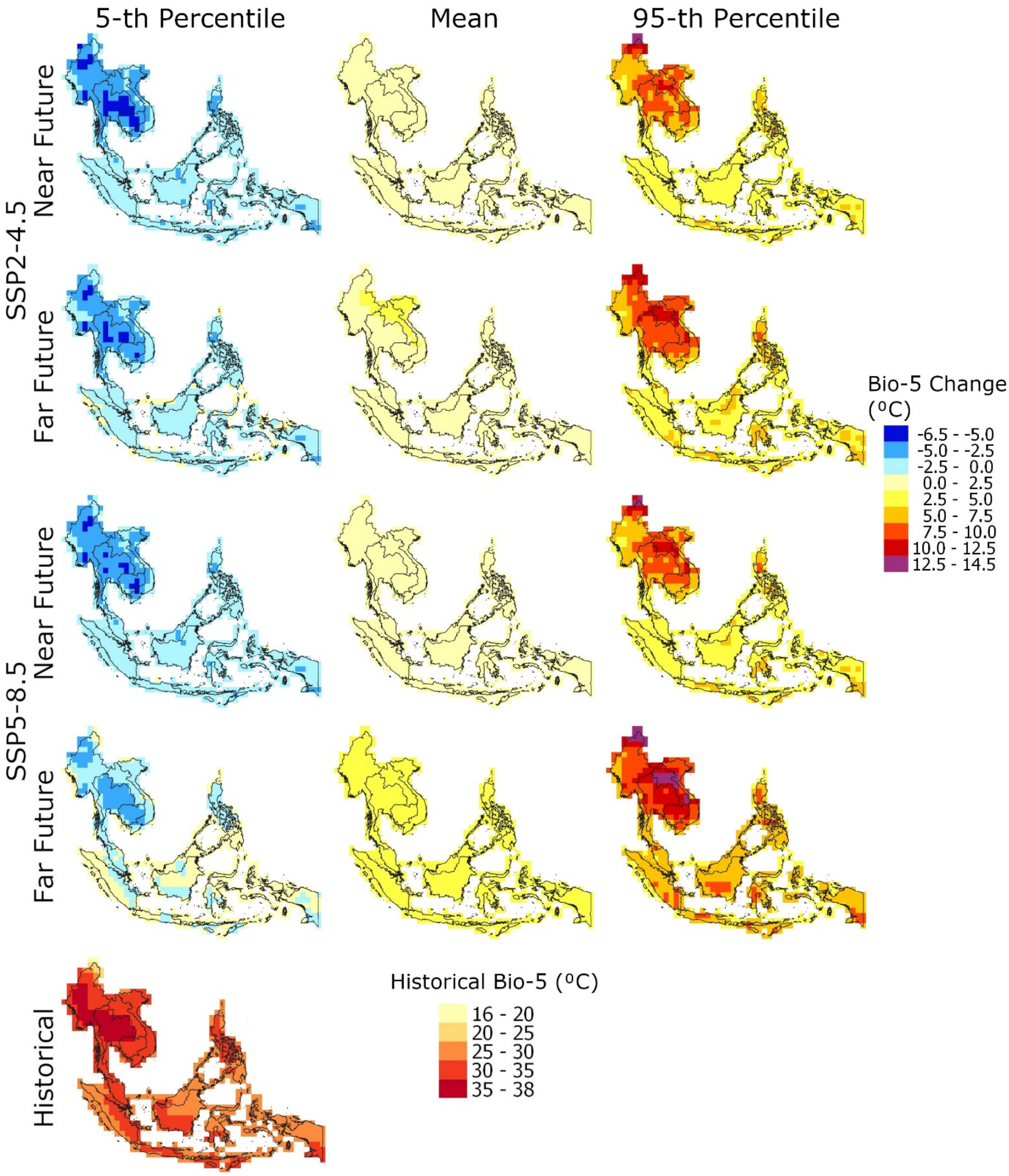

Fig. 6 Same as Figure 3 for the maximum temperature in warmest month (Bio-5)

4.6. Minimum temperature in the coldest month (Bio-6)

. Fig. 7 presents the minimum monthly temperature in the coldest month (Bio-6) over SEA, ranging between -17.0 and 27.0°C. The spatial distribution of Bio-6 was different from Bio-5 over SEA in many aspects. The lowest value was in the north (-17.0°C), and the highest in the coastal regions of Indonesia, Brunei, and the Philippines. The MME projected a mean change in Bio-6 by 1.06 and 1.88 °C for SSP2-4.5 and 1.27 and 3.15 °C for SSP5-8.5, for the near and far futures, respectively. The areal means of 5^{th} and 95^{th} percentiles of the projected changes for SSP2-4.5 were -1.39 and 3.50 °C for the near future, and -0.60 and 4.31 °C for the far future. Like Bio-5, the means of 5^{th} and 95^{th} percentiles of projection for SSP5-8.5 was the same as SSP2-4.5 during the near future. Nevertheless, in the far future, they were projected to increase by 0.69 and 5.69 °C for SSP5-8.5. North Myanmar would experience the lowest change in the 5^{th} percentile and the highest change in the 95^{th} percentile for all SSPs and future periods.

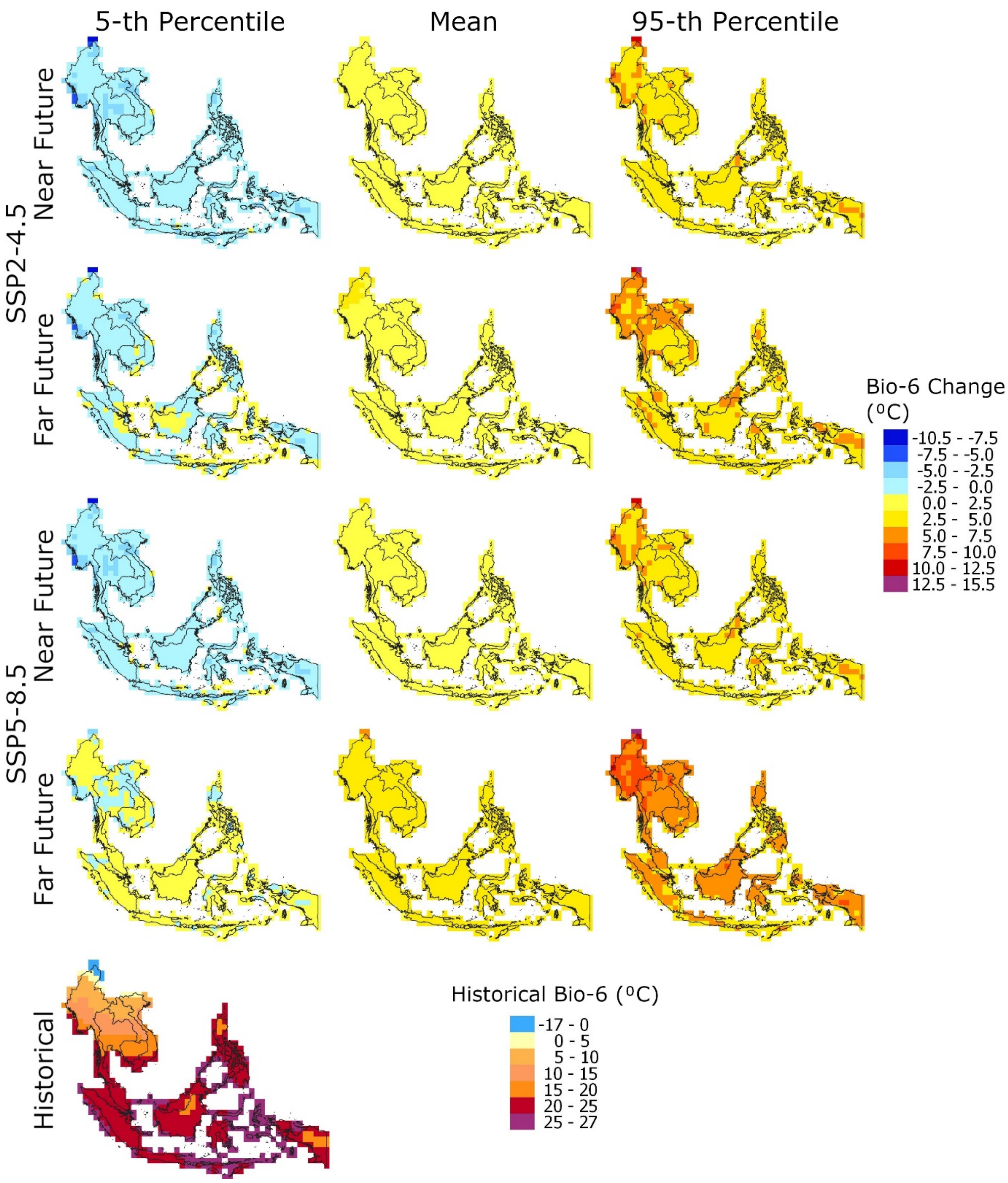

Fig. 7 Same as Figure 3 for minimum temperature in the coldest month (Bio-6)

4.7. Annual range of temperature (Bio-7)

Fig. 8 presents the annual temperature range (Bio-7) for historical and future scenarios in the SEA region. Bio-7 is the temperature variation during a certain period, which refers to the difference between Bio-5 and Bio-6. The spatial variability of Bio-7 was very high, between 2.0 and 33.0 °C, for SEA. The highest was in the north region (Myanmar, Thailand, Laos, and

Vietnam), and the lowest was in the southeast (North Maluku). The mean change in Bio-7 was projected between -1.00 and 0.65 °C in the near future and -1.83 and 0.73 °C in the far future for SSP2-4.5, while it was projected between -1.19 and 0.59 °C in the near future and -3.15 and 1.02 °C in the far future for SSP5-8.5. For SSP2-4.5, Bio-7 mean changes in the 5th percentile were -3.66 and -3.68 °C for the near and far future. The lowest change was in the SEA Mainland. The highest change in Bio-7 for the 95th percentile was also in the same region, between 0.50 and 9.74 °C for the near future and 0.43 and 9.63 °C for the far future. For SSP5-8.5, the areal means of 5th and 95th percentiles were -3.58 and 4.06 °C for the near future and -3.64 and 4.00 °C for the far future. The main change for each scenario and each future period was more in the north (SEA Mainland).

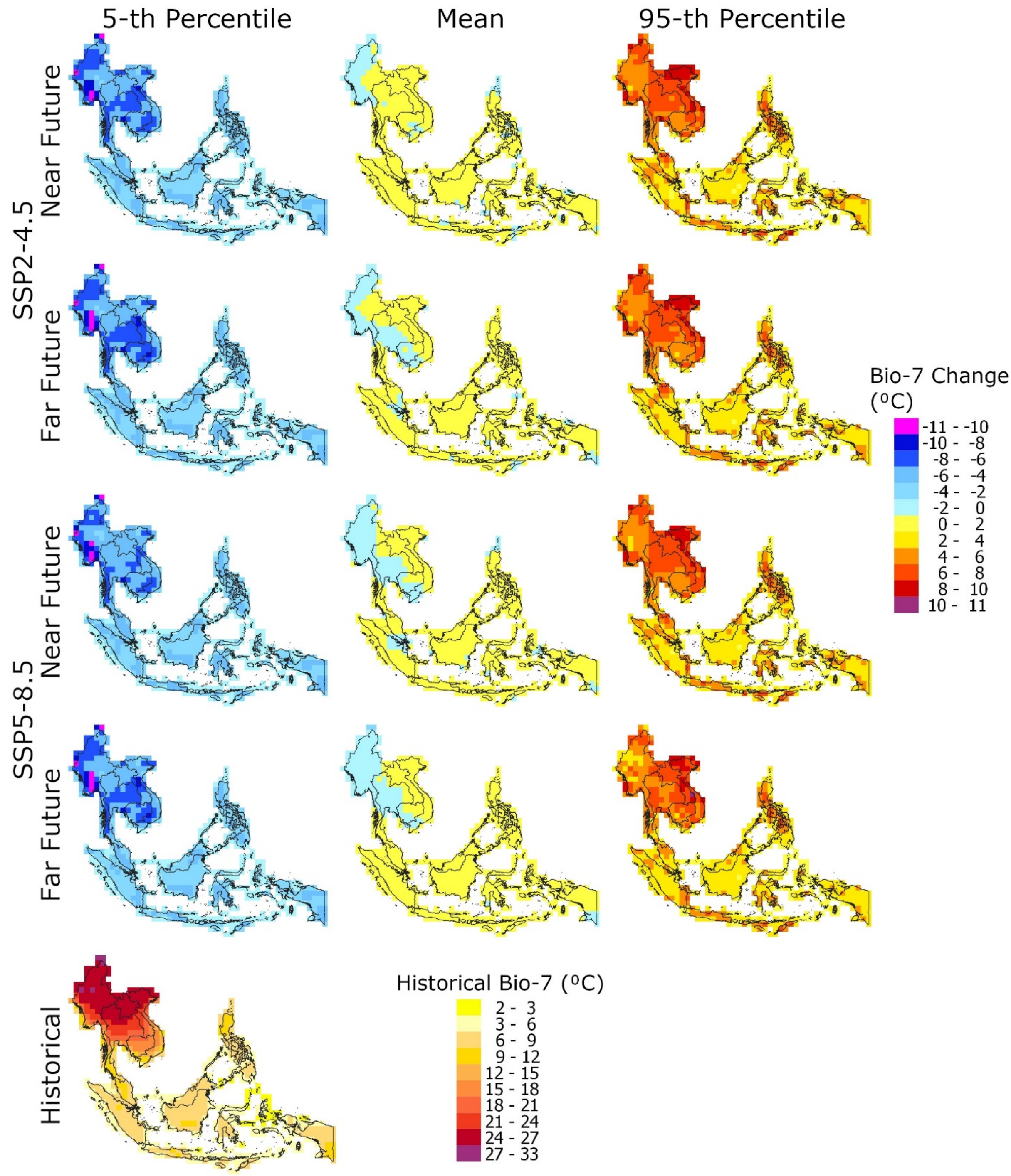

Fig. 8 Same as Figure 3 for annual temperature range (Bio-7)

4.8. Mean temperature of the wettest quarter (Bio-8)

Because the SEA region had a varied climate, the distribution of rainfall varies considerably throughout the year. As a result, the region's wettest quarter varies greatly. The wettest quarter for each grid point was calculated by the total rainfall over three consecutive months. Fig. 9 depicts the historical and projected mean temperature during the wettest quarter (Bio-8). The historical Bio-8 ranged between 9.0°C in the north of Myanmar and 29.0°C in the south of the region. The MME mean revealed that the mean changes in Bio-8 were expected to be 1.04 and 1.76 °C for the near and far futures for SSP2-4.5, while for SSP5-8.5, the changes were expected to be 1.21 and 2.97 °C for the near and far futures. For SSP2-4.5, the 5th percentile ranged between -5.26 and 0.04 °C in the near future, while in the far future, it ranged between -3.50 and 0.74 °C. The areal mean change of the 95th percentile was ranged between 1.78 and 6.81 °C in the near future and 2.83 and 6.77 °C in the far future. In the case of SSP5-8.5, the areal means of 5th and 95th percentile of the projected changes were estimated to be -0.55 and 3.32°C for the near future and 1.11 and 5.33°C for the far future.

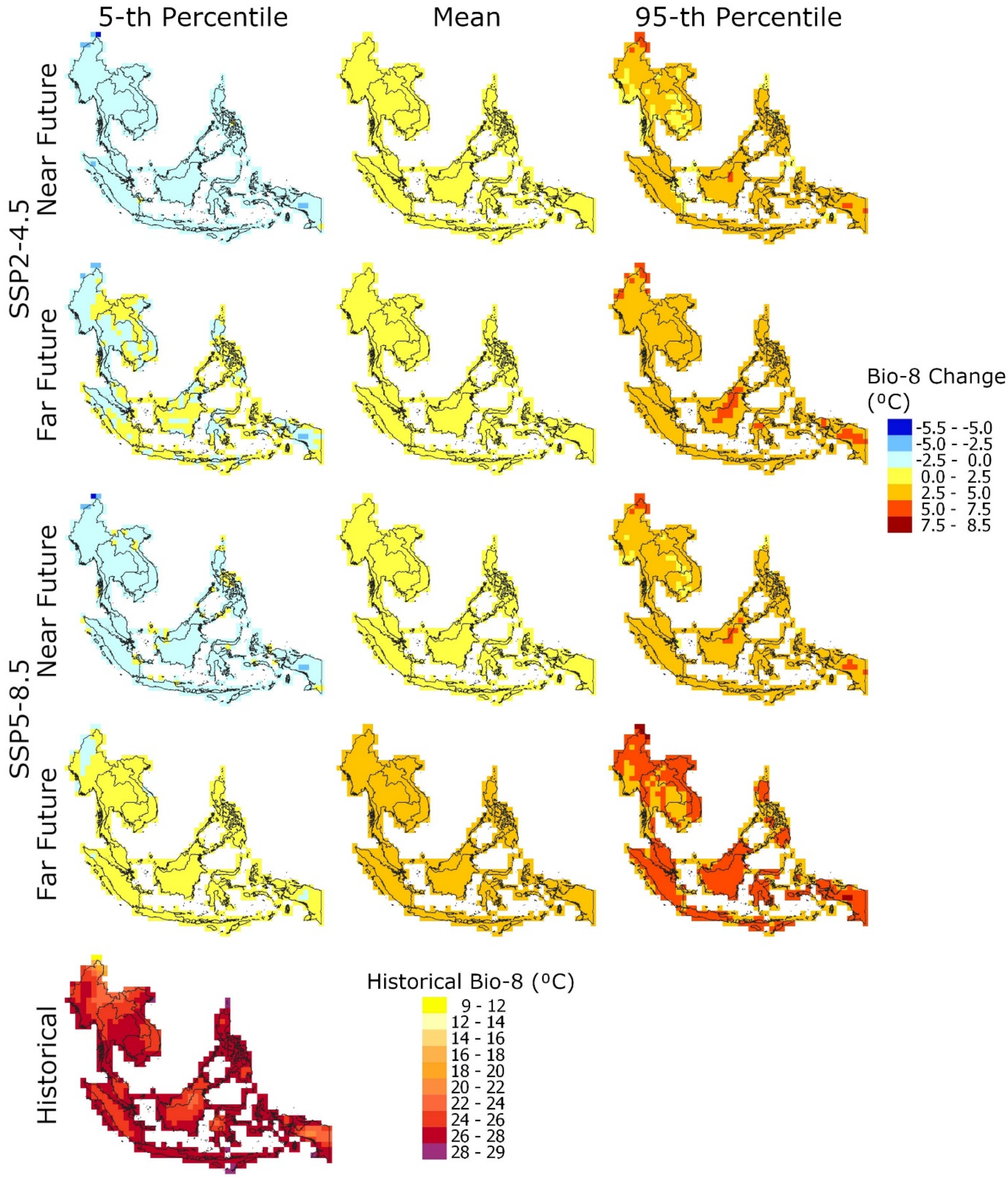

Fig. 9 Same as Figure 3 for the mean temperature of the wettest quarter (Bio-8)

4.9. Mean temperature of the driest quarter (Bio-9)

The rainfall for the three successive months was computed for each grid point to select the driest quarter. Fig. 10 illustrates the historical and future projection mean temperature through the driest quarter. During 1975 – 2014, the mean Bio-9 ranged between -6.0 and 28.0°C, where the lowest value in the north of Myanmar and the highest value distributed in coastal regions in the south. There were only three grids in the north region that contained historical Bio-9 less than 4.0°C. For SSP2-4.5, the MME mean change ranged between 0.51 and 2.10 °C during the near future and 1.13 and 3.54 °C during the far future. Bio-9 mean changes (5th percentile) were estimated to be -0.94 and -0.16 °C for the near and far future, with the lowest values in Myanmar. The 95th percentile changes were expected to be between 1.86 and 8.04 °C for the near future and 2.65 and 8.96 °C for the far future. For SSP5-8.5, the mean change of Bio-9 was ranged between 0.61 and 2.45 °C in the near future, while during the far future, it ranged between 1.98 and 5.80 °C. The areal means of the 5th and 95th percentiles were -0.72 and 3.87 °C for the near future and 1.01 and 5.97 °C for the far future.

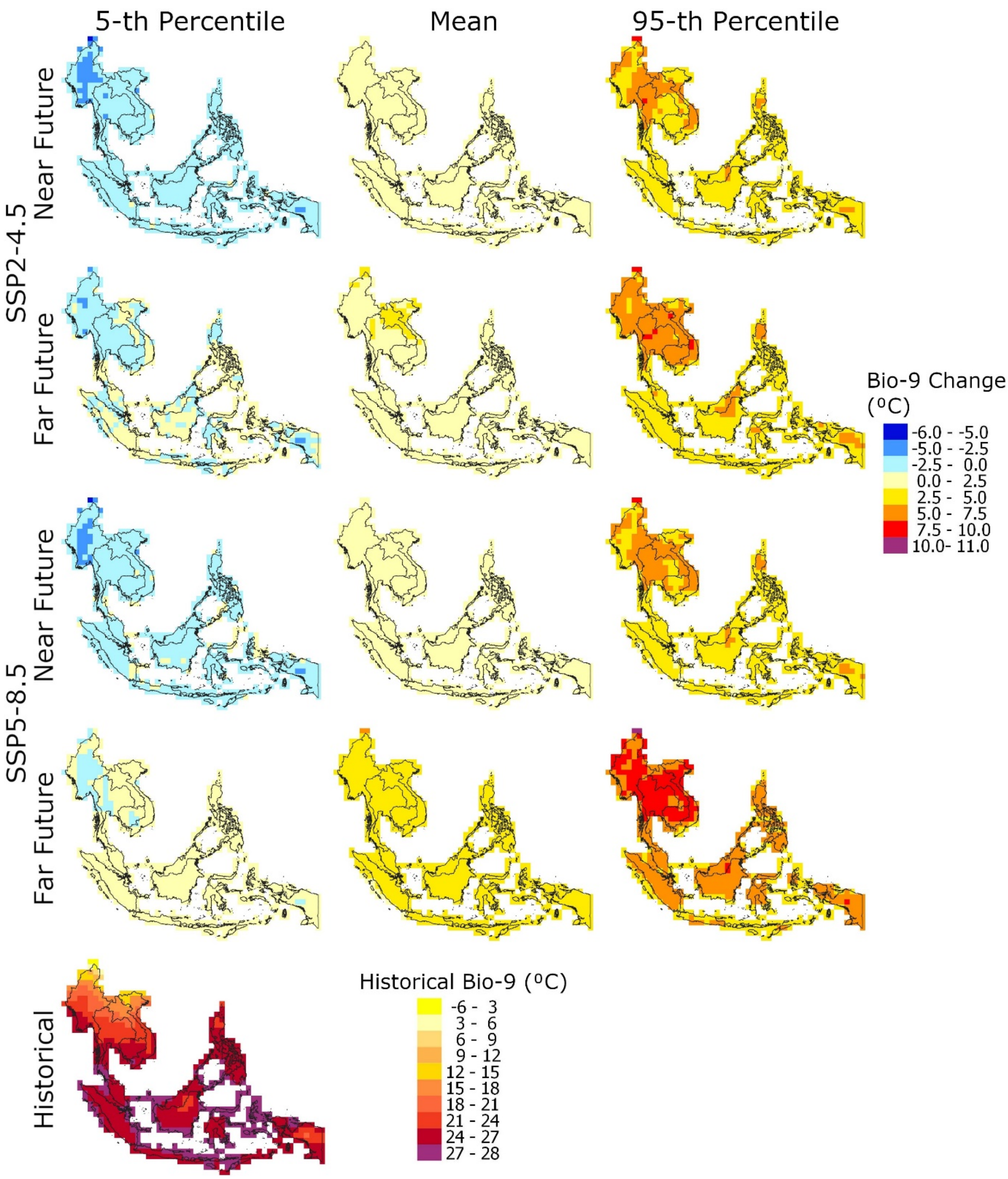

Fig. 10 Same as Figure 3 for the mean temperature of the driest quarter (Bio-9)

4.10. Mean temperature of the warmest quarter (Bio-10)

The mean temperature for the consecutive three months at each grid point was computed to determine the warmest quarter. Bio-10 is the average temperature calculated during the hottest quarter. Fig. 11 depicts the geographical distribution of Bio-10 and its projected changes over the SEA. The Bio-10 ranged between 11.0 and 29.0°C over SEA. The lowest value of Bio-10 was in the north, and the highest was along the coastal regions. The Bio-10 dispersion followed the geography of SEA. The mountains regions showed the lower Bio-10, while plains showed higher values. The mean future changes in Bio-10 was ranged between 0.87 and 1.61 °C in the near future, and 1.58 and 2.61 °C in the far future for SSP2-4.5, while it ranged between 1.03 and 1.77 °C in the near future and 2.70 and 4.08 °C in the far future for SSP5-8.5. For SSP2-4.5, Bio-10 mean changes (5^{th} percentile) were projected as -0.93 and -0.26 °C for the near and lowest change in the SEA Mainland for the far future. They were likewise in the 95^{th} percentile change in Bio-10, with a value between 2.07 and 7.05 °C in the near future and 2.93 and 8.52 °C in the far future. For SSP5-8.5, the projected 5^{th} and 95^{th} percentiles' means were -0.72 and 3.86 °C in the near future and 0.87 and 6.04 °C in the far future. The highest changes were projected in the north for all scenarios and future periods.

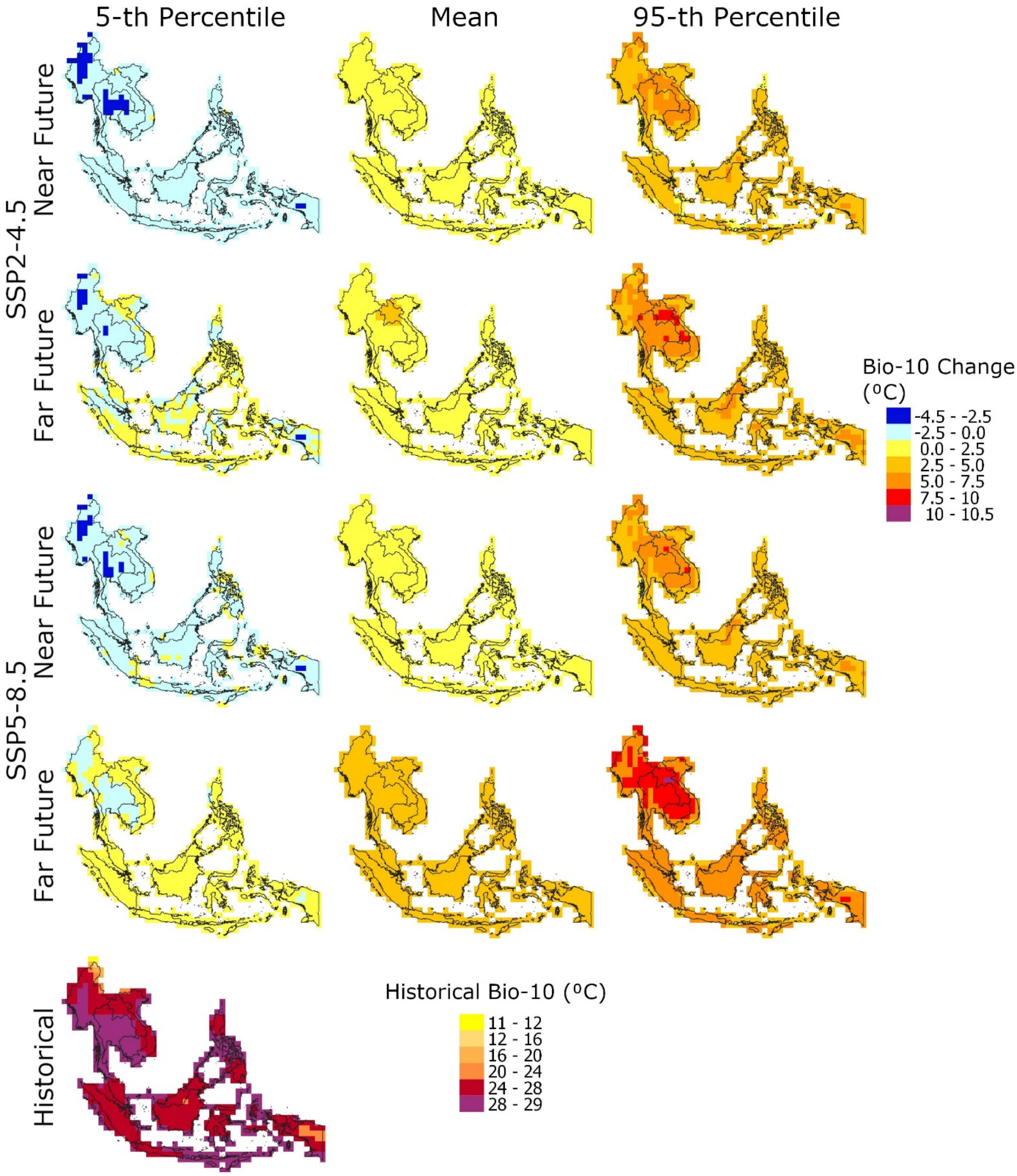

Fig. 11 Same as Figure 3 for the mean temperature of the warmest quarter (Bio-10)

4.11. Mean temperature of the coldest quarter (Bio-11)

The mean temperature over three consecutive months was computed at each grid point to get the coldest quarter. Bio-11 is the mean temperature of the coldest quarter. The spatial distribution of Bio-11 is presented in Fig. 12. The Bio-11 showed negative value only at two grids, while it ranged between zero and 27.0°C at other grids. The Bio-11 was lowest in the north of Myanmar and the highest in the coastal region of Indonesia. For SSP2-4.5, the MME projected the changes in Bio-11 by 1.06 and 1.84 °C in the near and far futures. The projected mean changes for SSP5-8.5 were 1.25 and 3.10 °C. The mean change in Bio-11 was like Bio-10, a similar increase in all future scenarios except for SSP5-8.5 in the far future. For SSP2-4.5, the anticipated mean change of 5^{th} and 95^{th} percentiles were -0.84 and 3.28 °C in the near future and -0.05 and 4.07 °C in the far future. There were no differences in the near future projections between SSP5-8.5 and SSP2-4.5. However, in the far future, the 5^{th} and 95^{th} percentiles mean changes were 1.16 and 5.45 °C, respectively.

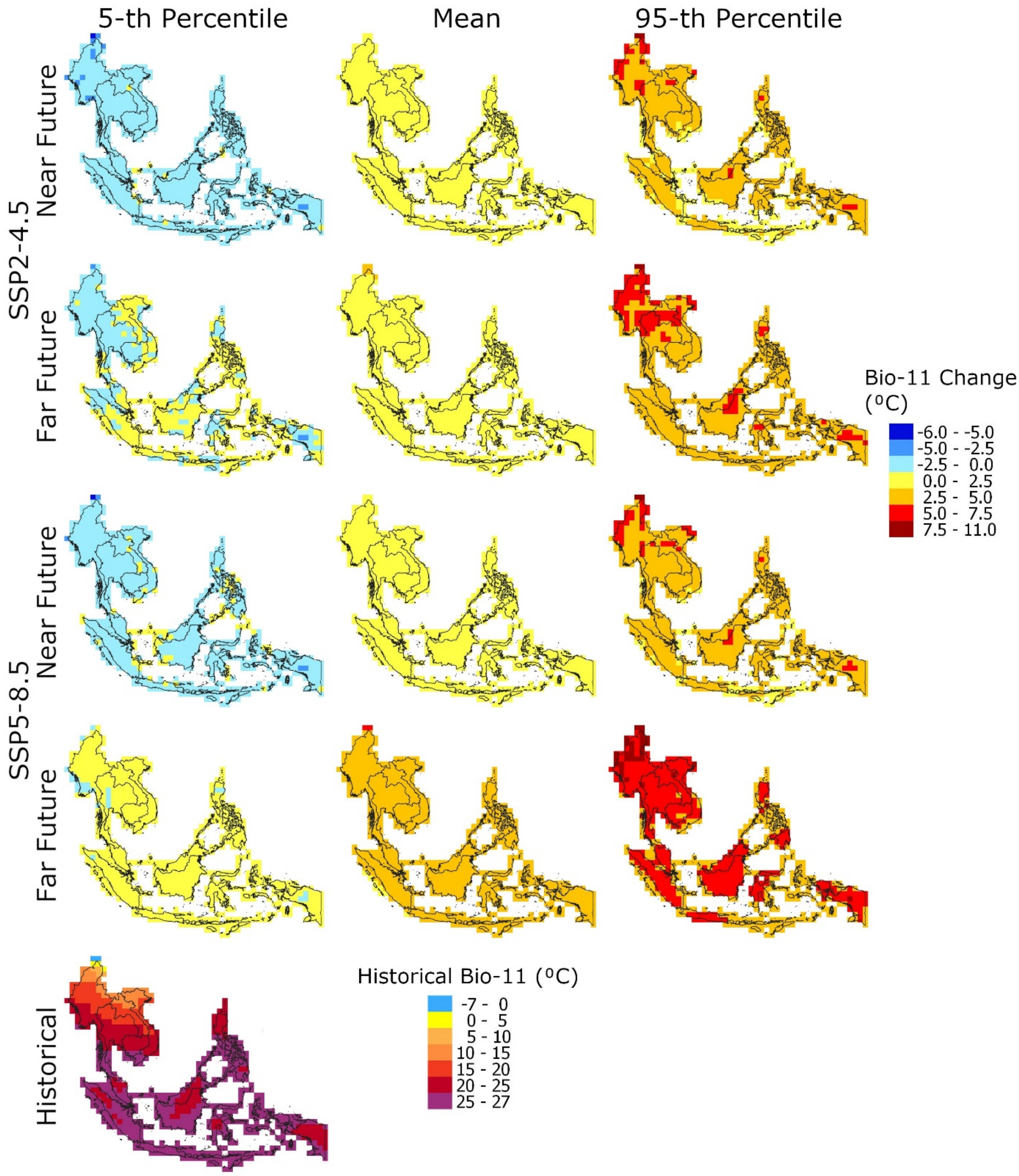

Fig. 12 Same as Figure 3 for the mean temperature of coldest quarter (Bio-11)

5. Conclusions

The present study assessed the geographical distribution of 11 thermal bioclimatic indicators in SEA and their possible spatiotemporal changes in the futures with associated uncertainty under medium and high climate change scenarios. The MME and 90% confidence interval of the projections of 23 GCMs were used. The study revealed an increase in mean and seasonal temperature over the whole SEA. However, the temperature would rise more in the warmest or wettest months compared to cold or dry months. This would cause an increase in the annual temperature range. A decrease in diurnal temperature range and increase in annual temperature range would cause a decrease in their ratio, and thus the isothermality. A decrease in seasonality at the same time may cause a shift in the climate in some parts of SEA. The environmental and conservation scientists can use the maps and information generated in this study to understand possible changes or shifts in biodiversity due to climate change. It can also be used by the governments of the region for sustainable development planning. Future studies can be conducted to evaluate the changes in other bioclimatic indicators related to rainfall and humidity. Besides, the species' sensitivity to the projected climate can be estimated to assess their risk and migration.

Funding

~~The authors did not receive support from any organization for the submitted work.~~

Conflicts of interest/Competing interests

We declare no conflict of interest.

Availability of data / Code

The datasets generated during and/or analyzed during the current study are available from the corresponding author on reasonable request.

Authors' contributions

All authors contributed to the study conception and design. Material preparation, data collection and analysis were performed by [Mohammed Magdy Hamed], [Mohammed Salem Nashwan] and [Shamsuddin Shahid]. The first draft of the manuscript was written by all authors.

References

Abdullah, M.T., 2003. Biogeography and variation of Cynopterus brachyotis in Southeast Asia. University of Queensland.

Almazroui, M., Saeed, F., Saeed, S., Nazrul Islam, M., Ismail, M., Klutse, N.A.B., Siddiqui, M.H., 2020. Projected Change in Temperature and Precipitation Over Africa from CMIP6. Earth Syst. Environ. 4, 455–475. https://doi.org/10.1007/s41748-020-00161-x

Asif, F., 2019. From Sea to City: Migration and Social Well-Being in Coastal Cambodia BT - Urban Climate Resilience in Southeast Asia, in: Daniere, A.G., Garschagen, M. (Eds.), The Urban Book Series. Springer International Publishing, Cham, pp. 149–177. https://doi.org/10.1007/978-3-319-98968-6_8

Banerjee, A.K., Mukherjee, A., Guo, W., Ng, W.L., Huang, Y., 2019. Combining ecological niche modeling with genetic lineage information to predict potential distribution of Mikania micrantha Kunth in South and Southeast Asia under predicted climate change. Glob. Ecol. Conserv. 20, e00800.

Bellard, C., Bertelsmeier, C., Leadley, P., Thuiller, W., Courchamp, F., 2012. Impacts of climate change on the future of biodiversity. Ecol. Lett. 15, 365–377. https://doi.org/10.1111/j.1461-0248.2011.01736.x

Boucher, O., Denvil, S., Levavasseur, G., Cozic, A., Caubel, A., Foujols, M.-A., Meurdesoif, Y., Cadule, P., Devilliers, M., Ghattas, J., Lebas, N., Lurton, T., Mellul, L., Musat, I., Mignot, J., Cheruy, F., 2018. IPSL IPSL-CM6A-LR model output prepared for CMIP6 CMIP. https://doi.org/10.22033/ESGF/CMIP6.1534

Çaliskan, O., Türkoglu, N., Matzarakis, A., 2013. The effects of elevation on thermal bioclimatic conditions in Uludağ (Turkey). Atmósfera 26, 45–57.

Cao, J., Wang, B., 2019. NUIST NESMv3 model output prepared for CMIP6 CMIP. https://doi.org/10.22033/ESGF/CMIP6.2021

Chai, Z., 2020. CAS CAS-ESM2.0 model output prepared for CMIP6 CMIP. https://doi.org/10.22033/ESGF/CMIP6.1944

Chen, H., Sun, J., Chen, X., 2014. Projection and uncertainty analysis of global precipitation-related extremes using CMIP5 models. Int. J. Climatol. 34, 2730–2748. https://doi.org/10.1002/joc.3871

Daham, A., Han, D., Matt Jolly, W., Rico-Ramirez, M., Marsh, A., 2018. Predicting vegetation phenology in response to climate change using bioclimatic indices in Iraq. J. Water Clim. Chang. 10, 835–851. https://doi.org/10.2166/wcc.2018.142

Dai, Y., Peng, G., Wen, C., Zahoor, B., Ma, X., Hacker, C.E., Xue, Y., 2021. Climate and land use changes shift the distribution and dispersal of two umbrella species in the Hindu Kush Himalayan region. Sci. Total Environ. 777, 146207. https://doi.org/10.1016/j.scitotenv.2021.146207

Deng, X., Perkins-Kirkpatrick, S.E., Lewis, S.C., Ritchie, E.A., 2021. Evaluation of Extreme Temperatures Over Australia in the Historical Simulations of CMIP5 and CMIP6 Models. Earth's Futur. 9, e2020EF001902. https://doi.org/10.1029/2020EF001902

Dix, M., Bi, D., Dobrohotoff, P., Fiedler, R., Harman, I., Law, R., Mackallah, C., Marsland, S., O'Farrell, S., Rashid, H., Srbinovsky, J., Sullivan, A., Trenham, C., Vohralik, P., Watterson, I., Williams, G., Woodhouse, M., Bodman, R., Dias, F.B., Domingues, C., Hannah, N., Heerdegen, A., Savita, A., Wales, S., Allen, C., Druken, K., Evans, B., Richards, C., Ridzwan, S.M., Roberts, D., Smillie, J., Snow, K., Ward, M., Yang, R., 2019. CSIRO-ARCCSS ACCESS-CM2 model output prepared for CMIP6 CMIP historical. https://doi.org/10.22033/ESGF/CMIP6.4271

Döscher, R., Acosta, M., Alessandri, A., Anthoni, P., Arneth, A., Arsouze, T., Bergmann, T., Bernadello, R., Bousetta, S., Caron, L.-P., Carver, G., Castrillo, M., Catalano, F., Cvijanovic, I., Davini, P., Dekker, E., Doblas-Reyes, F.J., Docquier, D., Echevarria, P., Fladrich, U., Fuentes-Franco, R., Gröger, M., v. Hardenberg, J., Hieronymus, J., Karami, M.P., Keskinen, J.-P., Koenigk, T., Makkonen, R., Massonnet, F., Ménégoz, M., Miller, P.A., Moreno-Chamarro, E., Nieradzik, L., van Noije, T., Nolan, P., O'Donnell, D., Ollinaho, P., van den Oord, G., Ortega, P., Prims, O.T., Ramos, A., Reerink, T., Rousset, C., Ruprich-Robert, Y., Le Sager, P., Schmith, T., Schrödner, R., Serva, F., Sicardi, V., Sloth Madsen, M., Smith, B., Tian, T., Tourigny, E., Uotila, P., Vancoppenolle, M., Wang, S., Wårlind, D., Willén, U., Wyser, K., Yang, S., Yepes-Arbós, X., Zhang, Q., 2021. The EC-Earth3 Earth System Model for the Climate Model Intercomparison Project 6. Geosci. Model Dev. Discuss. 2021, 1–90. https://doi.org/10.5194/gmd-2020-446

Duanmu, L., Sun, X., Jin, Q., Zhai, Z., 2017. Relationship between Human Thermal Comfort and Indoor Thermal Environment Parameters in Various Climatic Regions of China. Procedia Eng. 205, 2871–2878. https://doi.org/10.1016/j.proeng.2017.09.913

Eckstein, D., Künzel, V., Schäfer, L., 2017. Global climate risk index 2018. Ger. Bonn.

Ehbrecht, M., Schall, P., Ammer, C., Fischer, M., Seidel, D., 2019. Effects of structural heterogeneity on the diurnal temperature range in temperate forest ecosystems. For. Ecol. Manage. 432, 860–867. https://doi.org/10.1016/j.foreco.2018.10.008

Eyring, V., Bony, S., Meehl, G.A., Senior, C.A., Stevens, B., Stouffer, R.J., Taylor, K.E., 2016. Overview of the Coupled Model Intercomparison Project Phase 6 (CMIP6) experimental design and organization. Geosci. Model Dev. 9, 1937–1958. https://doi.org/10.5194/gmd-9-1937-2016

Flato, G., Marotzke, J., Abiodun, B., Braconnot, P., Chou, S.C., Collins, W., Cox, P., Driouech, F., Emori, S., Eyring, V., 2013. Climate change 2013: the physical science basis. contribution of working group i to the fifth assessment report of the intergovernmental panel on climate change. Eval. Clim. Model. eds TF Stock. D. Qin, G.-K. Plattner, M. Tignor, SK Allen, J. Boschung, al.(Cambridge Cambridge Univ. Press.

Hartmann, D.L., 2016. Chapter 11 - Global Climate Models, in: Hartmann, D.L.B.T.-G.P.C. (Second E. (Ed.), . Elsevier, Boston, pp. 325–360. https://doi.org/10.1016/B978-0-12-328531-7.00011-6

Hu, X.-G., Jin, Y., Wang, X.-R., Mao, J.-F., Li, Y., 2015. Predicting Impacts of Future Climate Change on the distribution of the Widespread Conifer Platycladus orientalis. PLoS One 10, e0132326.

Huang, W., 2019. THU CIESM model output prepared for CMIP6 CMIP historical. https://doi.org/10.22033/ESGF/CMIP6.8843

Karoly, D.J., Karl, B., Stott, P.A., Arblaster, J.M., Meehl, G.A., Broccoli, A.J., Dixon, K.W., 2003. Detection of a Human Influence on North American Climate. Science (80-.). 302, 1200–1203. https://doi.org/10.1126/science.1089159

Krasting, J.P., John, J.G., Blanton, C., McHugh, C., Nikonov, S., Radhakrishnan, A., Rand, K., Zadeh, N.T., Balaji, V., Durachta, J., Dupuis, C., Menzel, R., Robinson, T., Underwood, S., Vahlenkamp, H., Dunne, K.A., Gauthier, P.P.G., Ginoux, P., Griffies, S.M., Hallberg, R., Harrison, M., Hurlin, W., Malyshev, S., Naik, V., Paulot, F., Paynter, D.J., Ploshay, J., Reichl, B.G., Schwarzkopf, D.M., Seman, C.J., Silvers, L., Wyman, B., Zeng, Y., Adcroft, A., Dunne, J.P., Dussin, R., Guo, H., He, J., Held, I.M., Horowitz, L.W., Lin, P., Milly, P.C.D., Shevliakova, E., Stock, C., Winton, M., Wittenberg, A.T., Xie, Y., Zhao, M., 2018. NOAA-GFDL GFDL-ESM4 model output prepared for CMIP6 CMIP. https://doi.org/10.22033/ESGF/CMIP6.1407

Kriticos, D.J., Webber, B.L., Leriche, A., Ota, N., Macadam, I., Bathols, J., Scott, J.K., 2012. CliMond: Global high-resolution historical and future scenario climate surfaces for bioclimatic modelling. Methods Ecol. Evol. 3, 53–64. https://doi.org/10.1111/j.2041-210X.2011.00134.x

Kuo, C.-C., Gan, T.Y., Wang, J., 2020. Climate change impact to Mackenzie river Basin projected by a regional climate model. Clim. Dyn. 54, 3561–3581. https://doi.org/10.1007/s00382-020-05177-7

Molloy, S.W., Davis, R.A., Van Etten, E.J.B., 2014. Species distribution modelling using bioclimatic variables to determine the impacts of a changing climate on the western ringtail possum (Pseudocheirus occidentals; Pseudocheiridae). Environ. Conserv. 41, 176–186. https://doi.org/10.1017/S0376892913000337

Moss, R.H., Edmonds, J.A., Hibbard, K.A., Manning, M.R., Rose, S.K., van Vuuren, D.P., Carter, T.R., Emori, S., Kainuma, M., Kram, T., Meehl, G.A., Mitchell, J.F.B., Nakicenovic, N., Riahi, K., Smith, S.J., Stouffer, R.J., Thomson, A.M., Weyant, J.P., Wilbanks, T.J., 2010. The next generation of scenarios for climate change research and assessment. Nature 463, 747–756. https://doi.org/10.1038/nature08823

Nashwan, M.S., Ismail, T., Ahmed, K., 2018. Flood susceptibility assessment in Kelantan river basin using copula. Int. J. Eng. Technol. 7, 584–590. https://doi.org/10.14419/ijet.v7i2.8876

Nix, H.A., 1986. A biogeographic analysis of Australian elapid snakes. Atlas elapid snakes Aust. 7, 4–15.

O'Donnell, M.S., Ignizio, D.A., 2012. Bioclimatic Predictors for Supporting Ecological Applications in the Conterminous United States. U.S Geol. Surv. Data Ser. 691 10.

Ombadi, M., Nguyen, P., Sorooshian, S., Hsua, K., 2020. Retrospective Analysis and Bayesian Model Averaging of CMIP6 Precipitation in the Nile River Basin. J. Hydrometeorol. https://doi.org/10.1175/jhm-d-20-0157.1

Peano, D., Lovato, T., Materia, S., 2020. CMCC CMCC-ESM2 model output prepared for CMIP6 LS3MIP. https://doi.org/10.22033/ESGF/CMIP6.13165

Peel, M.C., Finlayson, B.L., McMahon, T.A., 2007. Updated world map of the Köppen-Geiger climate classificatio. Hydrol. Earth Syst. Sci. 11, 1633–1644. https://doi.org/10.1002/ppp.421

Pour, S.H., Wahab, A.K.A., Shahid, S., Wang, X., 2019. Spatial pattern of the unidirectional trends in thermal bioclimatic indicators in Iran. Sustain. 11. https://doi.org/10.3390/su11082287

Pu, Y., Liu, H., Yan, R., Yang, H., Xia, K., Li, Y., Dong, L., Li, L., Wang, H., Nie, Y., Song, M., Xie, J., Zhao, S., Chen, K., Wang, B., Li, J., Zuo, L., 2020. CAS FGOALS-g3 Model Datasets for the CMIP6 Scenario Model Intercomparison Project (ScenarioMIP). Adv. Atmos. Sci. 37, 1081–1092. https://doi.org/10.1007/s00376-020-2032-0

Ragheb, A.A., El-Darwish, I.I., Ahmed, S., 2016. Microclimate and human comfort considerations in planning a historic urban quarter. Int. J. Sustain. Built Environ. 5, 156–167. https://doi.org/10.1016/j.ijsbe.2016.03.003

Raitzer, D., Bosello, F., Tavoni, M., Orecchia, C., Marangoni, G., Samson, J., 2015. Southeast Asia and the economics of global climate stabilization. Asian Dev. Bank.

Rauff-Adedotun, A.A., Zain, S.N.M., Haziqah, M.T.F., 2020. Current status of Blastocystis sp. in animals from Southeast Asia: a review. Parasitol. Res. 1–12.

Rehfeldt, G.E., Worrall, J.J., Marchetti, S.B., Crookston, N.L., 2015. Adapting forest management to climate change using bioclimate models with topographic drivers. For. An Int. J. For. Res. 88, 528–539. https://doi.org/10.1093/forestry/cpv019

Ribeiro, M.M., Roque, N., Ribeiro, S., Gavinhos, C., Castanheira, I., Quinta-Nova, L., Albuquerque, T., Gerassis, S., 2019. Bioclimatic modeling in the Last Glacial Maximum, Mid-Holocene and facing future climatic changes in the strawberry tree (Arbutus unedo L.). PLoS One 14, e0210062.

Semmler, T., Danilov, S., Rackow, T., Sidorenko, D., Barbi, D., Hegewald, J., Sein, D., Wang, Q., Jung, T., 2018. AWI AWI-CM1.1MR model output prepared for CMIP6 CMIP 1pctCO2. https://doi.org/10.22033/ESGF/CMIP6.2543

Shahid, S., Harun, S. Bin, Katimon, A., 2012. Changes in diurnal temperature range in Bangladesh during the time period 1961–2008. Atmos. Res. 118, 260–270. https://doi.org/10.1016/j.atmosres.2012.07.008

Sintayehu, D.W., 2018. Impact of climate change on biodiversity and associated key ecosystem services in Africa: a systematic review. Ecosyst. Heal. Sustain. 4, 225–239. https://doi.org/10.1080/20964129.2018.1530054

Song, Z., Qiao, F., Bao, Y., Shu, Q., Song, Y., Yang, X., 2019. FIO-QLNM FIO-ESM2.0 model output prepared for CMIP6 CMIP historical. https://doi.org/10.22033/ESGF/CMIP6.9199

Swart, N.C., Cole, J.N.S., Kharin, V. V, Lazare, M., Scinocca, J.F., Gillett, N.P., Anstey, J., Arora, V., Christian, J.R., Hanna, S., Jiao, Y., Lee, W.G., Majaess, F., Saenko, O.A., Seiler, C., Seinen, C., Shao, A., Sigmond, M., Solheim, L., von Salzen, K., Yang, D., Winter, B., 2019. The Canadian Earth System Model version 5 (CanESM5.0.3). Geosci. Model Dev. 12, 4823–4873. https://doi.org/10.5194/gmd-12-4823-2019

Tatebe, H., Ogura, T., Nitta, T., Komuro, Y., Ogochi, K., Takemura, T., Sudo, K., Sekiguchi, M., Abe, M., Saito, F., Chikira, M., Watanabe, S., Mori, M., Hirota, N., Kawatani, Y., Mochizuki, T., Yoshimura, K., Takata, K., O'ishi, R., Yamazaki, D., Suzuki, T., Kurogi, M., Kataoka, T., Watanabe, M., Kimoto, M., 2019. Description and basic evaluation of simulated mean state, internal variability, and climate sensitivity in MIROC6. Geosci.

Model Dev. 12, 2727–2765. https://doi.org/10.5194/gmd-12-2727-2019

Taylor, K.E., Balaji, V., Hankin, S., Juckes, M., Lawrence, B., Pascoe, S., 2011. CMIP5 data reference syntax (DRS) and controlled vocabularies. San Francisco Bay Area, CA, USA.

Taylor, K.E., Stouffer, R.J., Meehl, G.A., 2012. An overview of CMIP5 and the experiment design. Bull. Am. Meteorol. Soc. 93, 485–498. https://doi.org/10.1175/BAMS-D-11-00094.1

Theusme, C., Avendaño-Reyes, L., Macías-Cruz, U., Correa-Calderón, A., García-Cueto, R.O., Mellado, M., Vargas-Villamil, L., Vicente-Pérez, A., 2021. Climate change vulnerability of confined livestock systems predicted using bioclimatic indexes in an arid region of México. Sci. Total Environ. 751, 141779.

van Vuuren, D.P., Edmonds, J., Kainuma, M., Riahi, K., Thomson, A., Hibbard, K., Hurtt, G.C., Kram, T., Krey, V., Lamarque, J.-F., Masui, T., Meinshausen, M., Nakicenovic, N., Smith, S.J., Rose, S.K., 2011. The representative concentration pathways: an overview. Clim. Change 109, 5. https://doi.org/10.1007/s10584-011-0148-z

van Zonneveld, M., Koskela, J., Vinceti, B., Jarvis, A., 2009. Impact of climate change on the distribution of tropical pines in Southeast Asia. Unasylva 60, 24–29.

Vinke, K., Schellnhuber, H.J., Coumou, D., Geiger, T., Glanemann, N., Huber, V., Kropp, J.P., Kriewald, S., Lehmann, J., Levermann, A., 2017. A region at risk: the human dimensions of climate change in Asia and the Pacific.

Volodin, E., Mortikov, E., Gritsun, A., Lykossov, V., Galin, V., Diansky, N., Gusev, A., Kostrykin, S., Iakovlev, N., Shestakova, A., Emelina, S., 2019a. INM INM-CM4-8 model output prepared for CMIP6 PMIP. https://doi.org/10.22033/ESGF/CMIP6.2295

Volodin, E., Mortikov, E., Gritsun, A., Lykossov, V., Galin, V., Diansky, N., Gusev, A., Kostrykin, S., Iakovlev, N., Shestakova, A., Emelina, S., 2019b. INM INM-CM5-0 model output prepared for CMIP6 CMIP piControl. https://doi.org/10.22033/ESGF/CMIP6.5081

von Storch, J.-S., Putrasahan, D., Lohmann, K., Gutjahr, O., Jungclaus, J., Bittner, M., Haak, H., Wieners, K.-H., Giorgetta, M., Reick, C., Esch, M., Gayler, V., de Vrese, P., Raddatz, T., Mauritsen, T., Behrens, J., Brovkin, V., Claussen, M., Crueger, T., Fast, I., Fiedler, S., Hagemann, S., Hohenegger, C., Jahns, T., Kloster, S., Kinne, S., Lasslop, G., Kornblueh, L., Marotzke, J., Matei, D., Meraner, K., Mikolajewicz, U., Modali, K., Müller, W., Nabel, J., Notz, D., Peters-von Gehlen, K., Pincus, R., Pohlmann, H., Pongratz, J., Rast, S., Schmidt, H., Schnur, R., Schulzweida, U., Six, K., Stevens, B., Voigt, A., Roeckner, E., 2017. MPI-M MPIESM1.2-HR model output prepared for CMIP6 HighResMIP. https://doi.org/10.22033/ESGF/CMIP6.762

Waltari, E., Schroeder, R., McDonald, K., Anderson, R.P., Carnaval, A., 2014. Bioclimatic variables derived from remote sensing: assessment and application for species distribution modelling. Methods Ecol. Evol. 5, 1033–1042. https://doi.org/10.1111/2041-210X.12264

Wang, A., Melton, A.E., Soltis, D.E., Soltis, P.S., 2021. Potential distributional shifts in North America of allelopathic invasive plant species under climate change models. Plant Divers. https://doi.org/10.1016/j.pld.2021.06.010

Wieners, K.-H., Giorgetta, M., Jungclaus, J., Reick, C., Esch, M., Bittner, M., Gayler, V., Haak, H., de Vrese, P., Raddatz, T., Mauritsen, T., von Storch, J.-S., Behrens, J., Brovkin, V., Claussen, M., Crueger, T., Fast, I., Fiedler, S., Hagemann, S., Hohenegger, C., Jahns, T., Kloster, S., Kinne, S., Lasslop, G., Kornblueh, L., Marotzke, J., Matei, D., Meraner, K., Mikolajewicz, U., Modali, K., Müller, W., Nabel, J., Notz, D., Peters-von Gehlen, K., Pincus, R., Pohlmann, H., Pongratz, J., Rast, S., Schmidt, H., Schnur, R., Schulzweida, U., Six, K., Stevens, B., Voigt, A., Roeckner, E., 2019. MPI-M MPI-ESM1.2-LR model output prepared for CMIP6 ScenarioMIP ssp245. https://doi.org/10.22033/ESGF/CMIP6.6693

Woetzel, J., Pinner, D., Samandari, H., 2020. Climate Risk and response. McKinsey Global Institute.

Wu, T., Chu, M., Dong, M., Fang, Y., Jie, W., Li, J., Li, W., Liu, Q., Shi, X., Xin, X., Yan, J., Zhang, F., Zhang, J., Zhang, L., Zhang, Y., 2018. BCC BCC-CSM2MR model output prepared for CMIP6 CMIP piControl. https://doi.org/10.22033/ESGF/CMIP6.3016

Yang, S., Wu, R., Jian, M., Huang, J., Hu, X., Wang, Z., Jiang, X., 2021. Climate Change in Southeast Asia and Surrounding Areas. Springer Climate.

Yoon, S., Lee, W.-H., 2021. Methodological analysis of bioclimatic variable selection in species distribution modeling with application to agricultural pests (Metcalfa pruinosa and Spodoptera litura). Comput. Electron. Agric. 190, 106430. https://doi.org/10.1016/j.compag.2021.106430

Yukimoto, S., Kawai, H., Koshiro, T., Oshima, N., Yoshida, K., Urakawa, S., Tsujino, H., Deushi, M., TANAKA, T., HOSAKA, M., YABU, S., YOSHIMURA, H., SHINDO, E., MIZUTA, R., OBATA, A., ADACHI, Y., ISHII, M., 2019. The Meteorological Research Institute Earth System Model Version 2.0, MRI-ESM2.0: Description and Basic Evaluation of the Physical Component. J. Meteorol. Soc. Japan. Ser. II 97, 931–965. https://doi.org/10.2151/jmsj.2019-051

Ziehn, T., Chamberlain, M., Lenton, A., Law, R., Bodman, R., Dix, M., Wang, Y., Dobrohotoff, P., Srbinovsky, J., Stevens, L., Vohralik, P., Mackallah, C., Sullivan, A., O'Farrell, S., Druken, K., 2019. CSIRO ACCESS-ESM1.5 model output prepared for CMIP6 CMIP. https://doi.org/10.22033/ESGF/CMIP6.2288